On the Coexistence of Broadcast and Unicast Networks for the Transmission of Video Services Using Stochastic Geometry

Ahmad Shokair, Youssef Nasser, Oussama Bazzi, Jean-François Hélard,
Matthieu Crussière

HAL Id: hal-01756820
https://hal.science/hal-01756820

Submitted on 4 Jun 2018

On the Coexistence of Broadcast and Unicast Networks for the Transmission of Video Services Using Stochastic Geometry

Ahmad Shokair, Youssef Nasser, Oussama Bazzi, Jean-Francois Hélard, and Matthieu Crussière,

Abstract—Following the increasing growth in the demand on mobile TV, hybrid broadcast/broadband networks emerged as a suitable approach to overtake the challenges introduced by each network separately in order to enhance users' experience. This paper presents two possible scenarios for a hybrid, spatially separated, broadcast/broadband network to offer mobile TV linear services for the end users. Namely, the first scenario is based on shared spectrum access for both networks while the second one proposes a dedicated spectrum. Using a stochastic geometry approach, the paper derives analytical formulations for both the probability of coverage and ergodic capacity. These formulations are then used to optimize the hybrid network in terms of its key design parameters including the Broadcast (BC) coverage radii, the Broadband (BB) Base Stations' (BS) density, and user satisfaction given in terms of spectral capacity. The results have shown that an optimal BC radius maximizing the probability of coverage and capacity exists and it depends on the BS density of the BB network. Other design parameters have been provided and analyzed leading to an optimal network deployment. To the best of the author's knowledge, this paper presents a first reference work dealing with the optimization of the hybrid network with the coexistence of broadband and broadcast networks, from stochastic geometry perspective, taking into account the inter-cell interference.

Index Terms—Mobile TV, Access network cooperation, broadcast networks, broadband networks, hybrid networks, network planning, LTE, DVB-T2, stochastic geometry.

I. INTRODUCTION

R ECENT years witnessed a high demand for linear services, especially mobile TV after the introduction of smartphones and tablets. This was made possible by the rapid advancement of both mobile-compatible Broadcast (BC) networks and mobile Broadband (BB) networks. However, the massive use of these smart devices has led to the extravagant use of BB resources leading to the so-called spectrum crisis. Recently, among the different solutions proposed in the literature, the co-existence between BC and BB networks has emerged as a possible solution dealing with band hungry applications, such as TV services. Therein, we firstly present the state-of-the-art technologies on linear services as well as the different existing approaches for coexistence.

A. Mobile TV

The market for mobile TV is primarily directed by the global increase in the adoption of live stream services. Mobile TV provides easy accessibility and availability of the desired video content provided by several platforms. Those factors encouraged consumers to prefer mobile TV over conventional TV. Other factors like the ability for a user to watch his favorite content for affordable prices also played a major role in the spread of this service. The penetration of advanced hand-held devices like smartphones and tablets made it even easier for mobile TV to spread, particularly in growing markets like India and China. Moreover, mobile TV has provided major revenues for mobile communication operators, TV providers, devices' manufacturers. Mainly, time and space flexibility, accessibility, cost efficiency and spread of platform are the main factors for the spread of mobile TV in the last few years. This will also continue in the next few years as reported in different references [1], [2].

In practice, Mobile TV could be delivered to the end-users in numerous methods. However, the latter could be grouped into two categories: wireless BC or BB mobile networks. Digital Video Broadcast (DVB) project developed several standards that could be compatible with the handheld devices including DVB-NGH in 2013, the successor to DVB-H in targeting handheld devices, and DVB-T2 in 2008, the second generation terrestrial video broadcast protocol which was designed to support both stationary and mobile devices [3]. In the US, Advanced Television System Committee (ATSC) adopted ATSC-M/H for hand-held mobile devices in 2009. ATSC 3.0 is the new version of ATSC standards, which is supposed to support mobile TV for Ultra High Definition (UHD) videos [4]. Other mobile TV compatible standards were also developed in different regions of the world, like ISDB-TMM a mobile-targeted version of the Integrated Services Digital Broadcasting (ISDB) in Japan in 2012 [5], Digital Terrestrial Multimedia Broadcast (DTMB) in China in 2006, and T-DMB by Digital Multimedia Broadcasting (DMB) in South Korea in 2007 [6].

From the BB perspective, mobile TV could be provided by different means. One way is to provide data by the regular mobile Unicast (UC) transmission. This method was made possible by the recent advances in wireless mobile networks in terms of rate spectral efficiency namely the 3rd Generation Partnership Project (3GPP) Long Term Evolution (LTE) [7]. Multicast is also possible in LTE since a special point-to-multipoint interface called, Multimedia BC Multicast Services (MBMS), has been firstly introduced by 3GPP network in 2002 and adopted by Universal Mobile Telecommunications System (UMTS) in 2011 [8], [9]. Evolved Multimedia Broadcast Multicast Services (eMBMS), an advanced version of MBMS has then been adopted by LTE. Contrarily to UC, eMBMS delivers content to multiple users through shared radio resources [10],

[11].

In practice, both networks i.e., BC and BB present their own limitations and advantages in terms of power, resources, performance, mobility, etc. Recently, hybrid networks based on the coexistence of BC and BB networks have emerged as a candidate solution to reach the required quality of service for the end-users, but this requires a thorough analysis and optimization of the transmission parameters.

B. Hybrid networks and related work

BC networks have a good cost and spectral efficiency for a large number of users, while this efficiency decays for lower user density [12]. Contrarily, BB UC networks maintain a good efficiency for a small number of users and suffer from overload due to limited spectral resources for a large number of users [13]. In addition, a BB base station has a limited coverage area due to path loss and power constraints, while the BB network provides wider coverage by means of multi-cells each with limited power. These facts encouraged the proposition of hybrid solutions, where BC and BB coexist to deliver linear services. A hybrid network could then be considered as an extension of the coverage area of the BC network by the help of the BB network. It could also be considered as the offloading of data traffic from the BB network to BC transmission.

In literature, several studies have been conducted on hybrid BB/BC networks, where the opportunities and challenges for the hybrid approach for current and future implementations were discussed in [12], [14], [15]. In general, one can classify the coexistence approaches into two main types: (1) hybrid collaboration within same-area networks and (2) spatially separated networks.

In same-area networks, authors in [16] proposed a system model, criteria, and constraints for load switching in hybrid cellular/BC network called switching bound concept. Heuck in [17] derived an analytical description of a hybrid network and an IP data-cast architecture and discussed its performance. Wang *et. al.* in [18] designed a push-based content delivery in a converged hybrid network to relieve the rapid growth in data traffic based on duration, popularity and size of the multimedia content. In [19], the authors proposed a converged BB/BC platform for delivering 3D media to fixed and mobile users guaranteeing a minimum QoS, alongside with an ideal business model for operators. Cornillet *et al.* studied the UC/BC cooperation from an energy point of view [20].Studies on the BC and BB coexistence from a spectral point of view, regarding overlapping and guard bands, were presented in [21] and [22]. Moreover, a unified BC layer targeting mobile devices, based on DVB-T2 and LTE/eMBMS standards, was proposed in [23]. Closely, the authors suggested in [24] an overlay over the UC network by the BC tower enabling cooperative spectrum usage.

On the other hand, in spatially separated networks, the authors of [25] proposed to maximize the global capacity for a hybrid BC/UC system in terms of power ratio between the BC tower and UC Base Station (BS), then derived a closed-form expression for ergodic capacity in the case of non-cooperative interfering coexistence. Authors in [26] planned a stand-alone DVB-NGH and LTE and studied the benefits from the cooperation between the two, then compared those scenarios from energy consumption perspective in [27]. In [13], a study on the service coverage of an extension scenario of a hybrid UC/BC network was proposed showing the existence of an optimal operation mode where global throughput is maximized. Fam *et al* then introduced an analytical model for the optimal coverage to maximize hybrid network system capacity in [28], provided a theoretical analysis of the hybrid network performance in [29] and studied the energy efficiency for such model in [30].

C. Stochastic geometry modeling

In the previous works, the BB part of the hybrid network was usually modeled with the traditional grid model. However, such model is not accurate in terms of BS density and distribution, especially in urban and suburban areas. Instead, recent studies have shown that stochastic geometry provides better, more realistic way of describing the distribution of a mobile network [31], [32]. In this approach, the position of BSs is set randomly using a point process. In fact, Poisson Point Process (PPP) provides a decent tool to model the BSs distribution with a single needed parameter, representing the average density of BSs in the service area [33]. PPP results in having, on average, the same number of points in a certain area A, wherever A is chosen along the service area, this number is equal to the product of the average density and the area A. In [34], the authors investigated the accuracy of this model by testing against real implemented BSs in the UK, concluding that the stochastic geometry based model is capable of modeling the network performance accurately. Andrews *et al* derived in [35] a general formula for the average probability of coverage and achievable throughput for a multi-cell BB network modeled by a PPP. The authors showed that a PPP is a pessimistic model compared to the conventional grid model, but is much more accurate in describing a real implementation, where the estimated coverage by a PPP is slightly below the actual coverage compared to the grid model which gives a higher estimate.

D. Contributions

This paper discusses the case of spatially separated hybrid BC/BB networks. However, since eMBMS is not yet widely deployed, this work considers a UC transmission for the BB network. Indeed, it was shown that UC could achieve significantly high coverage rates with a proper allocation of available resources [36]. In contrary to the previous works in [13], [28], [29], [30] where a grid model was used to describe the BB network, a more accurate PPP is used here to model BSs positions. Moreover, our work considers the Inter-Cell Interference (ICI) which has not been taken into account in the literature. The main contributions of this paper could be summarized as follows:

1) Proposition of a model for two deployment scenarios that could be used for a spatially separated hybrid network, *i.e.* users inside BC area are served by the BC tower, and the rest are served by nearest BB BS. The first scenario,

named shared spectrum scenario, considers that BB BSs outside BC area operate at the same frequency band as the BC. The second, named dedicated spectrum scenario, assumes that those BSs operate at other frequencies such as TV White Space (TVWS). Those scenarios are compared in terms of spectral efficiency.

2) Utilization of stochastic geometry tools by modeling the BS and users' positions of the BB network as PPP model.
3) Consideration of ICI as one of the most influential factors in the design and obtained results. The effect of interference cancellation is also studied.
4) Derivation of the analytical expressions that evaluate the average probability of coverage for BC users, BB UC users, and any user in the service area, for both scenarios. Similar derivations are provided for the user capacity at each position in the hybrid model.
5) Optimization of the hybrid network in terms of design parameters, especially the BC radius and the density of UC BSs.

The rest of this paper will be organized as follows. Section II describes both model architectures, in addition to the derivation of some important probability distribution functions (pdfs) that will be used in the following sections. Sections III & IV include the derivation for average coverage probability and average user capacity respectively, for both scenarios, and introduce some appropriate approximations when applicable. In section V, numerical simulations are conducted and compared to the analytical results. Then, a set of parameters is optimized to maximize the coverage and rate, besides studying the effect of interference cancellation on the performance. Finally, section VI draws the conclusion of the paper and suggests some future research directions.

II. PROPOSED SYSTEM MODEL AND SCENARIOS

In this section, we describe the hybrid network model including both transmission scenarios. In this work, we consider linear TV serviced to M users, distributed in a wide circular service area, resembling a typical metropolitan area, as shown in Fig. 1. The broadcast area is assumed to be occupying the center of the considered area. As for the broadband network, two main scenarios are considered. In the first scenario, UC BSs outside the broadcast area operate at the same frequency as the BC area, while in the second scenario, UC BSs operate at another band such as digital TV white space, so there is no interference between UC and BC networks. Each scenario presents its advantages and drawbacks in terms of spectrum allocation, interference level and hence system performance. Both approaches are in line with the current state-of-the-art considerations as detailed in the previous section.

The hybrid network consists of two Orthogonal Frequency Division Multiplexing (OFDM) systems:

1) A broadcasting system composed of a single High Power High Tower (HPHT) site located at the center of the service area.
2) A mobile broadband UC system composed of N_{BS} base station sites.

It is assumed that all the BB BSs transmit with the same power P_L, and the HPHT transmits with a power P_D such that

$$P_D > P_L$$

The BS are located according to a PPP Φ with a density λ_{BS} per squared Km. The users are distributed according to another, independent, PPP Ψ with a density equal to λ_u. It is also assumed that a user has the ability to connect to either system depending on its position, i.e. if the user is within the coverage area of the HPHT ($r_v < r_b$), then the user will be connected to it. Else, it will be outside the BC region hence connected to the nearest UC BS. This will result in a disk with broadcast users inside, and a Voronoi tessellation for UC users. An example of this network is shown in Fig. 1. For both transmission systems, the standard power loss propagation model is used, and it is assumed that all transmitter/receiver couples use Single Input Single Output (SISO) antennas.
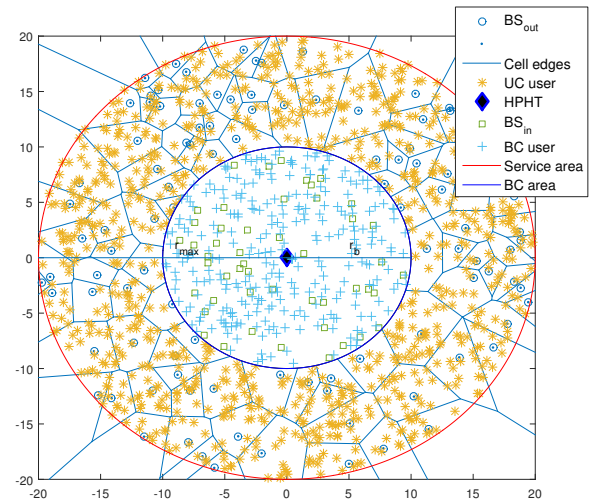

Fig. 1: An example of a service area, with 20 km radius, and 10 km broadcast radius

A. Scenario 1: shared spectrum scenario

In the first scenario, the BC network operates at frequency f_D, while UC operates at f_L for BSs within the BC area, and at f_D for BSs outside the BC domain. This is briefed in Fig. 2a. This arrangement will result in the following points:

(a) Inter-cell Interference for UC users concerns the outside area since the hybrid network is now operating at two different frequencies for inside and outside BS. The average level of interference for UC users depends on the ratio of broadcast area to the service area,
(b) Inside users fed by the HPHT suffer from interference from outside BS. However, this interference is variable depending on the distance from HPHT and can be significantly small for non-edge users.
(c) Outside users fed by the UC BSs suffer from interference from the HPHT. However, this interference is also variable depending on the distance from HPHT and can be significantly small especially if the broadcast area is large enough, and the power of HPHT is properly designed.

(d) The interest of this scheme is clearly seen in terms of bandwidth allocation as inside and outside users (of the broadcast area) with TV services are operating at the same frequency. This will be at the detriment of additional interference level as explained above.

The SINR for inside users is given by:

$$S_i = \frac{P_D g r_V^{-\beta}}{\sigma^2 + I_D} \tag{1}$$

where P_D is the transmission power by the HPHT, g represents the random channel effect between the HPHT and the user, including shadowing and fading. r_v is the distance between the HPHT and the user, β represents the path loss exponent for broadcast, σ^2 is the noise power, and I_D denotes the interference on an inside user from outside BS. The interference is the sum of the powers of the received interfering signals. For a user in the broadcast area operating at frequency f_D, all BSs in the UC area are considered as interferers, then I_D is given by:

$$I_D = \sum_{j \in \Phi} P_L \, h \, r_{s,j}^{-\alpha} \tag{2}$$

where P_L is the transmission power of UC BS, h represents the channel random effect between the BS and the user, $r_{s,j}$ is the distance between a user and interfering BS j and Φ is the set of all outside BS.

The SINR for outside users is given by:

$$S_o = \frac{P_L h r_l^{-\alpha}}{\sigma^2 + I_1 + I_2} \tag{3}$$

where r_l is the distance between the serving BS and the user, α represents the path loss exponent for UC, σ^2 is the noise power, and I_1 and I_2 denote the interference on an outside user from outside BS and the HPHT respectively. The interference on a user from interfering BS is given by:

$$I_1 = \sum_{j \in \Phi/b} P_L \, h \, r_{q,j}^{-\alpha} \tag{4}$$

and from the HPHT transmitter is given by:

$$I_2 = B_R P_D \, g \, r_d^{-\beta} \tag{5}$$

where Φ/b denotes the set of all BSs in the UC area excluding the serving BS for user under consideration. $r_{q,j}$ is the distance from an outside user and interfering BS j, and r_d is the distance from an inside user to the HPHT transmitter. B_r is the ratio between the BW of the BC and that of UC. Since in general, the bandwidth (BW) of the BB network is higher than that of the BC where both are overlapping, the ratio can be written as following:

$$B_R = min(1, \frac{BW_{BC}}{BW_{UC}}) \tag{6}$$

where BW_{BC} and BW_{UC} are the BW of BC and UC respectively.

B. Scenario 2: dedicated spectrum scenario

The second scenario considered in this paper differs from Scenario 1 in the spectrum allocation. Indeed, here the BC HPHT operates at f_D, UC BS inside BC area operate at f_L, while the BS outside BC domain operate at f_W, a sub-band of the TV white space, where f_L, f_W and f_D don't overlap. This scenario is summarized in Fig.2b. This will result in the following points:

(a) Compared to shared spectrum scenario, ICI for UC is significantly reduced due to the usage of three different frequencies.
(b) Contrarily to Scenario 1, inside users, fed by the HPHT will only be limited by path loss and noise, and will not suffer from any interference.
(c) Outside users fed by the UC BS suffer only from ICI produced by outside cells.
(d) The interference is limited at the expense of additional bandwidth allocation.

The SNR for inside users is given by:

$$S_i = \frac{P_D g r_V^{-\beta}}{\sigma^2} \tag{7}$$

The SINR for outside users is given by:

$$S_o = \frac{P_L h r_l^{-\alpha}}{\sigma^2 + I_1} \tag{8}$$

The difference from shared spectrum scenario is that I_D, the interference from outside BS on inside users, and I_2, the interference from HPHT on outside users, are both eliminated from the equations.

C. PDFs of main separation distances

Three distances shown in figure 3 are particularly important in the derivations that will follow: (1) the distance r_d between the UC user and the HPHT transmitter, (2) the distance r_v between a BC user and the center, and (3) the distance r_l between a UC user and its serving BS. Since both BS and users positions are random, those distances are random as well, and their distributions are needed in the derivation of coverage and capacity.

The CDF of r_d is given by:

$$\begin{aligned}
F_{r_d}(R_d) &= \mathbb{P}[r_d < R_d] \\
&= \frac{A(R_d, r_b)}{A_{UC}} \\
&= \frac{\pi R_d^2 - \pi r_b^2}{\pi r_{max}^2 - \pi r_b^2} \\
&= \frac{1}{r_{max}^2 - r_b^2} R_d^2 - \frac{r_b^2}{r_{max}^2 - r_b^2}
\end{aligned} \tag{9}$$

where $A(R_d, r_b)$ is the area limited by the two circles of radius R_d and r_b. The PDF of r_d will then be:

$$\begin{aligned}
f_{r_d}(R_d) &= \frac{dF_{r_d}(R_d)}{dR_d} \\
&= \frac{2}{r_{max}^2 - r_b^2} R_d
\end{aligned} \tag{10}$$

(a) Scenario 1: shared spectrum
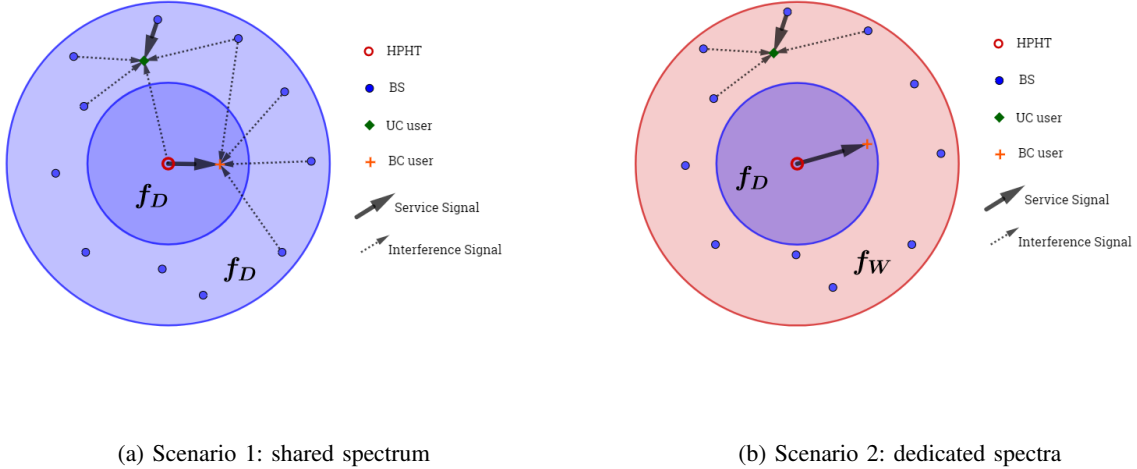
(b) Scenario 2: dedicated spectra
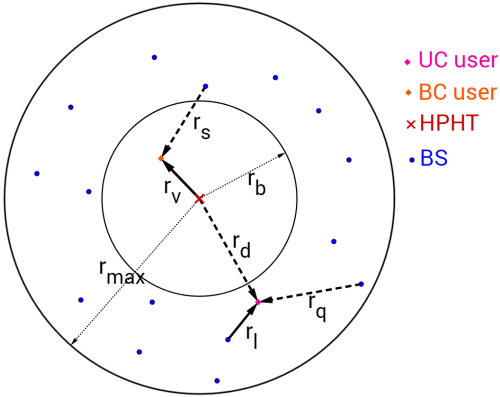
Fig. 2: Different proposed scenarios

Fig. 3: Important distances used in the model

Similarly, the PDF of r_v is given by:

$$f_{r_v}(R_v) = \frac{2}{r_b^2} R_v \qquad (11)$$

r_l represents the distance to the serving BS. That means that the area between the user and the serving BS is empty from any interfering BS. For a PPP in $\mathbb{R}^2$, the null probability in an area A is $\exp(-\lambda A)$ [35]. Then, the CCDF of r_l is as following:

$$
\begin{aligned}
F_{r_l}(R_l) &= \mathbb{P}[r_l < R_l] \\
&= 1 - \exp(-\lambda A) \\
&= 1 - \exp(-\lambda \int_{\max(r_b, r_d - R_l)}^{\min(r_{max}, r_d + R_l)} 2\theta v \, dv) \\
&= 1 - \exp(-2\lambda \int_{\max(r_b, r_d - R_l)}^{\min(r_{max}, r_d + R_l)} \arccos(\frac{v^2 + r_d^2 - R_l^2}{2v \, r_d}) v dv)
\end{aligned}
\qquad (12)
$$

Then, the PDF of r_l is given by:

$$f_{r_l}(R_l) = \frac{d}{dr_l}\left[exp\left(-2\lambda \int_{\max(r_b, r_d - R_l)}^{\min(r_{max}, r_d + R_l)} \arccos(\frac{v^2 + r_d^2 - R_l^2}{2v \, r_d}) v dv \right) \right] \qquad (13)$$

where the area A could be found as shown in Fig. 4.

Approximation of the PDF of r_l: Eq. (13) is very hard to express and interpret, and therefore will be hard to be used in the sequel. Alternately, it could be easily verified that if the edge cases are ignored, and the BS density exceeds a certain low-value threshold, the area to be processed is simpler, and could be seen as a complete disk with radius r_l. Thus the PDF of r_l could be reduced to:

$$f_{r_l}^*(R_l) = 2\pi\lambda r_l \exp(-\pi\lambda r_l^2) \qquad (14)$$

It can clearly be seen that even though the approximation is much simpler than the exact value, it completely ignores the relative position to the center and the broadcast radius r_b. In the sequel, this approximation will be used when necessary, like in the estimation of of average coverage probability for BC users in (17) and (32) and UC users in (23) and (34), where both the exact formula and the approximation could be used.

III. AVERAGE PROBABILITY OF COVERAGE

In this section, we derive the analytical expressions for the average probability of coverage of inside users (i.e. broadcast region), outside users (i.e. UC region), and the average probability of coverage of any user at any position. The probability of coverage is defined as the probability of a user to have a SINR value higher than a certain threshold T [35]. In order to clarify the derivation steps, Table I summarizes the used symbols. Since shared spectrum scenario and dedicated spectrum scenario have slight differences in the derivation of final expressions, the derivation for the first scenario is explained, while in the second scenario, only the final result is stated with indication on the differences.
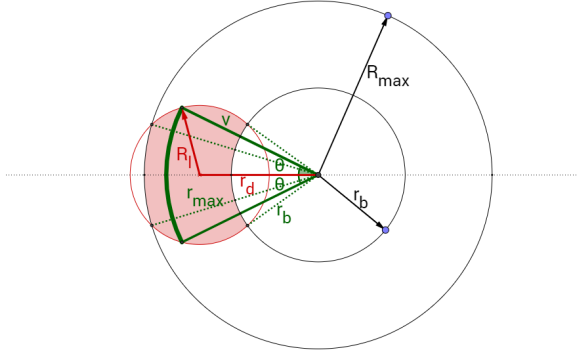
Fig. 4: Calculation of area limited by the circle of radius R_l, service area circle, and broadcast area circle

TABLE I: Table of used symbols

Symbol	indication
r_{max}	Radius of service area
r_b	Radius of BC area
r_l	Distance from user under UC to serving BS
r_d	Distance from user under UC HPHT
r_q	Distance from user under UC to interfering BS
r_v	Distance from user under BC to HPHT
r_s	Distance from user under BC to interfering BS
P_D	Tx power of HPHT
P_L	Tx power of BS
g	Term including random HPHT-user channel conditions
h	Term including random BS-user channel conditions
α	Path loss exponent for BS and a user
β	Path loss exponent for HPHT and a user
σ^2	Noise power at the receiver
λ_{BS}	Density of BS PPP
λ_u	Density of users PPP
T	SINR threshold
P_c	Probability of coverage for a general user
$P_{c/i}$	Probability of coverage for a BC user
$P_{c/o}$	Probability of coverage for a UC user
C	Capacity per Hz for a general user
C_i	Capacity per Hz for a BC user
C_o	Capacity per Hz for a UC user

A. Shared Spectrum Scenario

1) Coverage for BC users: For inside users under broadcast, the average probability of coverage is given by:

$$
\begin{aligned}
P_{c/i} &= \mathbb{E}_{r_v}\left[\mathbb{P}(S_i > T/r_v)\right] \\
&= \mathbb{E}_{r_v}\left[\mathbb{P}\left(\frac{P_D g r_V^{-\beta}}{\sigma^2 + I_D} > T/r_v\right)\right] \\
&\overset{(a)}{=} \int_0^{r_b} \mathbb{P}\left(g > \frac{T r_V^\beta}{P_D}(\sigma^2 + I_D)/r_v\right) f_{r_v}(r_v) dr_v \\
&= \frac{2}{r_b^2} \int_0^{r_b} \mathbb{P}\left(g > \frac{T r_V^\beta}{P_D}(\sigma^2 + I_D)/r_v\right) r_v dr_v
\end{aligned}
\tag{15}
$$

where (a) follows the independence of the distribution of r_v and the channel g. Here, we can derive:

$$
\begin{aligned}
\mathbb{P}\left(g > \frac{T r_V^\beta}{P_D}(\sigma^2 + I_D)/r_v\right) &= \mathbb{E}_{I_D}\left[\mathbb{P}\left(g > \frac{T r_V^\beta}{P_D}(\sigma^2 + I_D)/I_D, r_v\right)\right] \\
&\overset{(b)}{=} \mathbb{E}_{I_D}\left[exp\left(\frac{-\tau T r_V^\beta}{P_D}(\sigma^2 + I_D)\right)\right] \\
&= exp\left(\frac{-\tau T r_V^\beta \sigma^2}{P_D}\right)\mathbb{E}_{I_D}\left[exp\left(\frac{-\tau T r_V^\beta}{P_D} I_D\right)\right] \\
&= exp\left(\frac{-\tau T r_V^\beta \sigma^2}{P_D}\right)\mathscr{L}_{I_D}\left(\frac{-\tau T r_V^\beta}{P_D}\right)
\end{aligned}
\tag{16}
$$

where (b) follows the assumption of an exponential distribution of g: $g \sim exp(\tau)$. $\mathscr{L}_{I_D}(s)$ is the Laplace transform of I_D evaluated at s. Then:

$$
P_{c/i} = \frac{2}{r_b^2} \int_0^{r_b} exp\left(\frac{-\tau T r_V^\beta \sigma^2}{P_D}\right)\mathscr{L}_{I_D}\left(\frac{-\tau T r_V^\beta}{P_D}\right) r_v dr_v
\tag{17}
$$

The exact derivation for the Laplace transform $\mathscr{L}_{I_D}(s)$ results in the following formula:

$$
\begin{aligned}
\mathscr{L}_{I_D}\left(\frac{\tau T r_v^\beta}{P_D}\right) = \exp\Bigg(-2\lambda\Bigg(&\int_0^{r_{max}-r_v} \frac{\pi r_s}{1 + \frac{\mu P_D r_s^\alpha}{T \tau P_L r_b^\beta}} dr_s \\
&+ \int_{r_{max}-r_v}^{r_{max}+r_v} \frac{\arccos\left(\frac{r_v^2 + r_s^2 - r_{max}^2}{2 r_v r_s}\right)}{1 + \frac{\mu P_D r_s^\alpha}{T \tau P_L r_b^\beta}} r_s dr_s \\
&- \int_0^{r_b - r_v} \frac{\pi r_s}{1 + \frac{\mu P_D r_s^\alpha}{T \tau P_L r_b^\beta}} dr_s \\
&- \int_{r_b-r_v}^{r_b+r_v} \frac{\arccos\left(\frac{r_v^2 + r_s^2 - r_b^2}{2 r_v r_s}\right)}{1 + \frac{\mu P_D r_s^\alpha}{T \tau P_L r_b^\beta}} r_s dr_s\Bigg)\Bigg)
\end{aligned}
\tag{18}
$$

It is very clear that Eq.(18) could be reduced to simple closed-form expressions, hence two different approximations are provided as follows.

Approximation 1 of Eq.(18): Here, it is assumed that due to high BC transmission power, interference is not effective beyond certain point, so the effective interference could be reduced to the disk surrounding a user, with a radius equal to the distance of HPHT from that user. In this case, (18) can be written as:

$$
\mathscr{L}_{I_D}^*\left(\frac{\tau T r_v^\beta}{P_D}\right) = \exp\left(-2\lambda \int_{r_b-r_v}^{min(r_{max}-r_v, r_v)} \frac{\pi - \arccos\left(\frac{r_v^2 + r_s^2 - r_{max}^2}{2 r_v r_s}\right)}{1 + \frac{\mu P_D r_s^\alpha}{T \tau P_L r_b^\beta}} r_s dr_s\right)
\tag{19}
$$

Approximation 2 of Eq.(18): A second approximation could be obtained by assuming that interference is produced by a single interferer placed on the closest point to a user directly on the BC/UC border. This approximation is not generally accurate, but it significantly reduces the complexity of the calculations. The Laplace transform yields:

$$
\mathscr{L}_{I_D}^{**}\left(\frac{\tau T r_v^\beta}{P_D}\right) = \frac{1}{1 + \frac{\tau P_L T r_V^\beta}{\mu P_D (r_b - r_v)^\alpha}}
\tag{20}
$$

The derivations of the Laplace transform, and the approximations could be found in Appendix B.

Eq.(17) indicates, as expected, that increasing the radius of BC area without a suitable increase in broadcast power will decrease the average coverage probability for BC users especially for edge users with a high value of r_v causing both terms inside the integral to be significantly smaller. In fact, the second approximation shown in (19) indicates that the BC radius r_b has a significant additional effect since it appears in the denominator with an exponent which is higher than 2. The equations also indicate that increasing the BS transmission power P_L will reduce the coverage for BC users, with the BS's density λ has a similar effect.

2) Coverage for UC users: Outside users are connected to the nearest BS, operating at f_D, and served using unicast. Those users suffer from two sources of interference due to the HPHT power and the other outside BSs. The probability of coverage of the outside users could be written as:

$$
\begin{aligned}
P_{c/o} &= \mathbb{E}_{r_d, r_l}\Big[\mathbb{P}[S_o > T/r_d, r_l]\Big] \\
&= \mathbb{E}_{r_d, r_l}\Big[\mathbb{P}\big[\frac{P_L h r_l^{-\alpha}}{\sigma^2 + I_1 + I_2} > T/r_d, r_l\big]\Big] \\
&= \int_{r_b}^{r_{max}} f_{r_d}(r_d) \int_0^{2r_{max}} f_{r_l}(r_l)\mathbb{P}[h > \frac{Tr_l^\alpha}{P}(\sigma^2 + I_1 + I_2)/r_d, r_l] dr_l dr_d
\end{aligned}
$$

(21)

where the last step follows the independence of the distribution of r_d, r_l and the channel random effect represented by h. The distance r_d between an outside user and the HPHT varies between r_b in the case of a user on the edge of the broadcast area, and r_{max} in the case of a user on the edge of the service area. On the other hand, r_l, the distance between an outside user and its serving base station, varies between zero and $2r_{max}$. However, practically the upper limit is likely much less, especially when the BS density is high enough. Again, the probability of coverage for outside users can be deduced from the previous equation by:

$$
\begin{aligned}
&\mathbb{P}[h > \frac{Tr_l^\alpha}{P}(\sigma^2 + I_1 + I_2)/r_d, r_l] \\
&= \mathbb{E}_{I_1}\Big[\mathbb{E}_{I_2}\big[\exp\big(\frac{-\mu Tr_l^\alpha}{P_L}(\sigma^2 + I1 + I2)\big)\big]\Big] \\
&= \exp\big(\frac{-\mu Tr_l^\alpha \sigma^2}{P_L}\big)\mathscr{L}_{I_1/r_d}\big(\frac{\mu Tr_l^\alpha}{P_L}\big)\mathscr{L}_{I_2/r_d}\big(\frac{\mu Tr_l^\alpha}{P_L}\big)
\end{aligned}
$$

(22)

where the first step follows the independence of the interference from HPHT and the interference from surrounding BSs, and follows also the exponential distribution of the channel parameter h: $h \sim exp(\mu)$. Plugging this into (21), and substituting $f_{r_d}(r_d)$ by its formula derived in (10), we get:

$$
\begin{aligned}
P_{c/o} &= \frac{2}{r_{max}^2 - r_b^2} \int_{r_b}^{r_{max}} r_d \int_0^{r_{max}} f_{r_l}(r_l)\exp\big(\frac{-\mu Tr_l^\alpha \sigma^2}{P_L}\big) \\
&\quad \mathscr{L}_{I_1/r_d, r_l}\big(\frac{\mu Tr_l^\alpha}{P_L}\big)\mathscr{L}_{I_2/r_d, r_l}\big(\frac{\mu Tr_l^\alpha}{P_L}\big) dr_l dr_d
\end{aligned}
$$

(23)

$\mathscr{L}_{I_1/r_d}\big(\frac{\mu Tr_l^\alpha}{P_L}\big)$ and $\mathscr{L}_{I_2/r_d}\big(\frac{\mu Tr_l^\alpha}{P_L}\big)$ are the Laplace transform of I_1 and I_2 respectively. $\mathscr{L}_{I_1/r_d}(s)$ can be evaluated at cer-

tain values of r_l and r_d. The exact derivations, reported in Appendix C, lead to the following formula:

$$
\begin{aligned}
\mathscr{L}_{I_1/r_d}\big(\frac{\mu Tr_l^\alpha}{P_L}\big) = \exp\Bigg(&-2\lambda\Big(\int_{min(r_l, r_{max}-r_d)}^{r_{max}-r_d} \frac{\pi r_q}{1 + \frac{1}{T}\big(\frac{r_q}{r_l}\big)^\alpha} dr_q \\
&+ \int_{max(r_l, r_{max}-r_d)}^{r_{max}+r_d} \frac{\arccos(\frac{r_d^2 + r_q^2 - r_{max}^2}{2r_d r_q})}{1 + \frac{1}{T}\big(\frac{r_q}{r_l}\big)^\alpha} r_q dr_q \\
&- \int_{max(r_l, r_d - r_b)}^{r_d + r_b} \frac{\arccos(\frac{r_d^2 + r_q^2 - r_b^2}{2r_d r_q})}{1 + \frac{1}{T}\big(\frac{r_q}{r_l}\big)^\alpha} r_q dr_q\Big)\Bigg)
\end{aligned}
$$

(24)

Approximation of the LT in (24): In order to reduce the complexity of (24), an approximation could be made, by assuming that the major source of interference is due to the first term which represents the disk limited by the BC disk and the service area circle. From the above formula, this will lead the following:

$$
\mathscr{L}_{I_1/r_d}^*\big(\frac{\mu Tr_l^\alpha}{P_L}\big) = \exp\Bigg(-2\lambda\int_{min(r_l, r_{max}-r_d)}^{r_{max}-r_d} \frac{\pi r_q}{1 + \frac{1}{T}\big(\frac{r_q}{r_l}\big)^\alpha} dr_q\Bigg)
$$

(25)

On the other hand, $\mathscr{L}_{I_2/r_d}(s)$ could be evaluated for certain values of r_d as follows:

$$
\begin{aligned}
\mathscr{L}_{I_2/r_d}(s) &= \mathbb{E}_g\Big[\exp(-sI_2)\Big] \\
&= \mathbb{E}_g\Big[\exp(-sB_R P_D g r_d^{-\beta})\Big] \\
&= \frac{1}{1 + \frac{sB_R P_D r_d^{-\beta}}{\tau}}
\end{aligned}
$$

(26)

then

$$
\mathscr{L}_{I_2/r_d}\big(\frac{\mu Tr_l^\alpha}{P_L}\big) = \frac{1}{1 + \frac{B_R T\mu P_D r_d^{-\beta} r_l^\alpha}{\tau P_L}}
$$

(27)

From the three terms in (24) or from the approximation made in (25) one can conclude that the UC transmission power doesn't affect the Laplace transform of the inter-cell interference. However, increasing P_L boosts the overall coverage by increasing the other two terms in (23). Moreover, taking into account the approximations done in (14) and (25), the effect of the BS density λ is not similarly clear. From one point, increasing λ_{BS} increases the linear part in (14), but decreases the exponential parts in (14) and (25). Thus the overall effect of λ_{BS} depends on other factors that appear in the exponential and control the decay rate like T and α. Note that for the case of B_r equal to 0, indicating no overlapping, the equation returns to the case where no interference from the BC on the UC exists, and $\mathscr{L}_{I_2/r_d}\big(\frac{\mu Tr_l^\alpha}{P_L}\big)$ is meaningless, and the coverage probability will be similar to that scenario 2, which will be later shown in (34).

3) Coverage for any user in the service area: Since the users are randomly and uniformly distributed over the service area, then the probability of a user to be in the broadcast region is

$$P_i = \frac{A_{BC}}{A_{total}} \quad (28)$$
$$= \frac{r_b^2}{r_{max}^2}$$

where A_{BC} is the BC area, and A_{total} is the service area. Consequently, the probability of a user to be in the UC region domain is

$$P_o = 1 - \frac{r_b^2}{r_{max}^2} \quad (29)$$

and the total probability of coverage for a general user in the service area will be

$$P_c = P_i P_{c/i} + P_o P_{c/o} \quad (30)$$

B. Dedicated Spectrum Scenario

The derivation steps of Scenario 2 are similar to that of Scenario 1 with one major difference: the elimination of I_D and I_2 and their related equations. Thus the probability of coverage for inside users will be as follows:

$$P_{c/i} = \frac{2}{r_b^2} \int_0^{r_b} \exp\left(\frac{-\mu T r_V^\beta \sigma^2}{P_D}\right) r_v dr_v \quad (31)$$

using equation 3.381/8 in [37] this equation could be written in the form:

$$P_{c/i} = \frac{2}{r_b^2} \frac{\gamma\left(\frac{2}{\beta}, \frac{\mu T \sigma^2 r_b^\beta}{P_D}\right)}{\beta\left(\frac{\mu T \sigma^2}{P_D}\right)^{2/\beta}} \quad (32)$$

where $\gamma(a,x)$ is the incomplete gamma function given by:

$$\gamma(a,x) = \int_0^\infty e^{-v} v^{a-1} dv \quad (33)$$

In addition, the probability of coverage of outside users could be written as :

$$P_{c/o} = \frac{2}{r_{max}^2 - r_b^2} \int_{r_b}^{r_{max}} r_d \int_0^{r_{max}} f_{r_l}(r_l) \exp\left(\frac{-\mu T r_l^\alpha \sigma^2}{P_L}\right)$$
$$\mathscr{L}_{I_1/r_d}\left(\frac{\mu T r_l^\alpha}{P_L}\right) dr_l dr_d \quad (34)$$

In Scenario 2, one can notice that coverage of inside users is related only to the parameters of the BC, and it is independent of the unicast parameters. In addition, the coverage of outside users is dependent only on UC parameters and r_b. This means that in general, the coverage of inside and outside users will increase with this model, but at the expense of using an additional frequency band.

IV. AVERAGE CAPACITY DERIVATION

In this section, we consider the average capacity for a bandwidth unit. As in the previous section, derivations for scenario 1 are described, and the final results of the second scenario follow.

A. Shared Spectrum Scenario

We consider the average capacity for a bandwidth unit to be as follows:

$$C = \log_2[1 + SINR] \quad (35)$$

1) Capacity for inside users: the average capacity for the inside users served by broadcast can be evaluated as:

$$C_i = \mathbb{E}[\log_2(1 + S_i)]$$
$$= \mathbb{E}_{\Phi,g}[\log_2(1 + \frac{P_D g r_V^{-\beta}}{\sigma^2 + I_D})]$$
$$= \int_0^{r_b} f_{r_v}(r_v) \mathbb{E}\left[\log_2(1 + \frac{P_D g r_V^{-\beta}}{\sigma^2 + I_D})/r_v\right] dr_v$$
$$\stackrel{(a)}{=} \int_0^{r_b} f_{r_v}(r_v) \int_0^\infty \mathbb{P}\left[\log_2(1 + \frac{P_D g r_V^{-\beta}}{\sigma^2 + I_D}) > t/r_v\right] dt dr_v$$
$$= \int_0^{r_b} f_{r_v}(r_v) \int_0^\infty \mathbb{P}\left[g > \frac{(2^t - 1) r_V^\beta}{P_D}(\sigma^2 + I_D)/r_v\right] dt dr_v$$
$$= \int_0^{r_b} f_{r_v}(r_v) \int_0^\infty \mathbb{E}_{I_D}\left[\exp\left(\frac{-\tau(2^t - 1) r_V^\beta}{P_D}(\sigma^2 + I_{D/r_v})\right)\right] dt dr_v$$
$$= \frac{2}{r_b^2} \int_0^{r_b} r_v \int_0^\infty \exp\left(\frac{-\tau(2^t - 1) r_V^\beta \sigma^2}{P_D}\right) \mathscr{L}_{I_D}\left(\frac{\tau(2^t - 1) r_V^\beta}{P_D}\right) dt dr_v$$
$$\quad (36)$$

where (a) follows from

$$\mathbb{E}[X] = \int_0^\infty \mathbb{P}(X > x) dx \quad (37)$$

$\mathscr{L}_{I_D}(s)$ is calculated in Appendix B. It could be used by substituting s by $\frac{\tau(2^t - 1) r_V^\beta}{P_D}$.

2) Capacity for outside users: Using similar analysis, the average capacity for outside users is given by:

$$C_o = \mathbb{E}_{r_d, r_l, h}\left[\log_2(1 + S_o)\right]$$
$$= \int_{r_b}^{r_{max}} f_{r_d}(r_d) \int_0^{2r_{max}} f_{r_l}(r_l) \mathbb{E}\left[\log_2\left(1 + \frac{P_L h r_l^{-\alpha}}{\sigma^2 + I_1 + I_2}\right)/r_d, r_l\right] dr_l dr_d$$
$$\stackrel{(a)}{=} \int_{r_b}^{r_{max}} f_{r_d}(r_d) \int_0^{2r_{max}} f_{r_l}(r_l) \int \mathbb{P}\left[\log_2\left(1 + \frac{P_L h r_l^{-\alpha}}{\sigma^2 + I_1 + I_2}\right) > t/r_d, r_l\right] dt dr_l dr_d$$
$$= \int_{r_b}^{r_{max}} f_{r_d}(r_d) \int_0^{2r_{max}} f_{r_l}(r_l) \int_0^\infty \mathbb{P}\left[h > \frac{(2^t - 1) h r_l^\alpha}{P_L}(\sigma^2 + I_1 + I_2)/r_d, r_l\right] dt dr_l dr_d$$
$$\stackrel{(b)}{=} \int_{r_b}^{r_{max}} f_{r_d}(r_d) \int_0^{2r_{max}} f_{r_l}(r_l) \int_0^\infty \mathbb{E}_{I_1, I_2}\left[\exp\left(\frac{-\mu(2^t - 1) r_l^\alpha}{P_L}(\sigma^2 + I_1 + I_2)\right)/r_d, r_l\right] dtd$$
$$= \frac{2}{r_{max}^2 - r_b^2} \int_{r_b}^{r_{max}} r_d \int_0^{2r_{max}} f_{r_l}(r_l) \int_0^\infty \exp\left(\frac{-\mu(2^t - 1) r_l^\alpha \sigma^2}{P_L}\right)$$
$$\mathscr{L}_{I_1/r_d}\left(\frac{\mu(2^t - 1) r_l^\alpha}{P_L}\right) \mathscr{L}_{I_2/r_d}\left(\frac{\mu(2^t - 1) r_l^\alpha}{P_L}\right) dt dr_l dr_d$$
$$\quad (38)$$

where (a) also follows from (37), and (b) follows the exponential distribution of h. The final step follows the independence between I_1 and I_2.

3) Total average capacity: Similar to the probability of coverage of a user at any position, the average capacity will be

$$C = P_i C_i + P_o C_o \tag{39}$$

B. Dedicated Spectrum Scenario

In scenario 2, the capacity for inside and outside users are similar to that of model 1, but again, with the elimination of terms related to I_D and I_2. The capacity of inside users could then be derived and written as:

$$C_i = \frac{1}{\ln(2)} \frac{2}{r_b^2} \int_0^{r_b} r_v \int_0^{\infty} \exp\left(\frac{-\tau(e^t-1)r_V^{\beta}\sigma^2}{P_D}\right) dt dr_v \tag{40}$$

By some rearrangement, and the use of equation 3.327 in [37], the capacity can be written as:

$$C_i = \frac{1}{\ln(2)} \frac{2}{r_b^2} \int_0^{r_b} r_v \exp\left(\frac{\tau\sigma^2 r_v^{\beta}}{P_D}\right)\left[-E_i\left(-\frac{\tau\sigma^2 r_v^{\beta}}{P_D}\right)\right] dr_v \tag{41}$$

where $E_i(x)$ is the exponential integral function given by:

$$E_i(x) = -\int_{-x}^{\infty} \frac{e^{-u}}{u} du \tag{42}$$

Moreover, the capacity for outside users is given by:

$$C_o = \frac{2}{r_{max}^2 - r_b^2} \int_{r_b}^{r_{max}} r_d \int_0^{2r_{max}} f_{r_l}(r_l) \int_0^{\infty} \exp\left(\frac{-\mu(2^t-1)r_l^{\alpha}\sigma^2}{P_L}\right)$$
$$\mathscr{L}_{I_1/r_d}\left(\frac{\mu(2^t-1)r_l^{\alpha}}{P_L}\right) dt dr_l dr_d \tag{43}$$

C. Effective Capacities

All previously calculated capacities are per frequency unit. However, to derive the average user capacity, multiplication by the occupied bandwidth is needed. But for the BC users, the average effective capacity is related to the transmitted bit rate, which is the required capacity for a proper reception of the service or C^{req}. Hence, the total BC capacity is given by:

$$C^{BC} = \sum_{m \in \mathscr{M}} C^{req} a_m \tag{44}$$

where $\mathscr{M}$ is the set of users within BC region, and a_m a binary variable that is equal to 1 if the SINR for user m named $SINR_m$ is greater or equal to the threshold T and 0 otherwise, thus indicating if user m is receiving the service properly or not.

The average BC capacity in the broadcast area could be then calculated as follows:

$$[C^{BC}] = C^{req} P_{c/i} \lambda_U \pi r_b^2 \tag{45}$$

where $\lambda_U \pi r_b^2$ is equal to the average number of users inside BC area.

Similarly, for UC users, the total cell capacity is given by:

$$C_n^{UC,cell} = \sum_{m \in \mathscr{C}_n} C_m^{user} b_{m,n} \tag{46}$$

where $\mathscr{C}_n$ is the set of users in the cell, C_m^{user} is the capacity for user m, and b_m is a binary variable that is equal to 1 if user m is connected to the service *i.e.* $SINR_m > T$. C_m^{user} could be found as follows:

$$C_m^{user} = N_m^{RB} B^{RB} \log_2(1 + SINR_m) \tag{47}$$

where N_m^{RB} is the number of resource blocks allocated to user m, and B^{RB} is the bandwidth of a single resource block. So for the UC network, the total capacity will be:

$$C^{UC} = \sum_{n \in \mathscr{N}} C_n^{UC,cell} \tag{48}$$

Thus, the average UC capacity could be derived as:

$$[C^{UC}] = [N^{RB}] B^{RB} C_o P_{c/o} \lambda_U \pi (r_{max}^2 - r_b^2) \tag{49}$$

where $\lambda_U \pi (r_{max}^2 - r_b^2)$ sums the average number of UC users, and $[N^{RB}]$ denotes the average number of resource blocks assigned for a user. Finally the total average capacity could be given as:

$$[C^{sys}] = [C^{BC}] + [C^{UC}] \tag{50}$$

Those values are used to derive the capacity of the hybrid system for both scenarios.

V. SIMULATION RESULTS

To compare the formulations derived previously with simulations, numerical and Monte-Carlo (MC) simulations have been conducted. Numerical analysis was also used to find optimal operating points for different of system parameters. The service area selected is of 30 km radius, with variable BC radius. Unless otherwise mentioned, the density of BSs is equal to $0.15 BS/km^2$. Default simulation settings are summarized in Table II. The isotropic transmission power of BSs is set to 1200 W, and the isotropic transmission power of the HPHT is set to 33 kW.

TABLE II: Simulation setting

Parameter	Value
r_{max}	30 km
r_b	10 km
P_D	33 kW
P_L	1.2 kW
BW_{BC}	8 MHz
BW_{UC}	10 MHz
μ	1
τ	1
α	3.4
β	3.2
σ^2	-100 dBm
λ_{BS}	$0.15 BS/km^2$
λ_u	$1 user/km^2$
T	0 dB

A. Simulation and analytical results in terms of coverage CCDF

Firstly, to compare the analytical expressions with MC simulation results, the CCDF of the probability of coverage is calculated for inside users, outside users, and any user in the service area as shown in Fig. 5a, 5b, and 5c respectively for shared spectrum scenario, and in Fig. 6a, 6b, and 6c respectively for dedicated spectra scenario.

Both Fig. 5a and 6a show a very good convergence between the simulation and the analytical results. Fig. 5b and 6b show a very high accuracy as well, with error ranging from 1 to 2%. Fig.5c and 6c verify the derived formulations and the different probability expressions in the previous sections. The first approximation for BC users presented in equation (19), and the approximation for UC users provided by Eq. (25) produce very close values to both simulation results and derived equations. The second approximation for the BC users provided by Eq. (19) is accurate for high threshold values, and looses its accuracy for low threshold values, *i.e.* below $3dB$. However, the use of these approximations reduces significantly the processing time for the analytical derivations. Fortunately, these approximations work well with the practical transmission parameters.

The problem turns out now to find the optimal set of parameters which maximizes the probability of coverage and users' capacity.

B. Optimization of the Hybrid Network

Among the different design parameters, it is very clear that the first parameter to optimize is the radius (i.e. the coverage) of the broadcast area for both scenarios. Fig. 7a and 7b show the probability of coverage vs the BC radius for a general user in the service area for UC BS densities of $0.05BS/km^2$ and $0.15BS/km^2$ for both scenarios. The results show that for a small value of r_b, where most users are UC users, the probability of coverage P_c will be limited by the achievable P_c in the UC network. When the BC radius r_b increases, more users are being covered by the BC network and thus the total P_c increases. However, when r_b is increased too much, edge users associated with BC become out of coverage due to high interference, pathloss and noise levels. Optimal values of r_b vary between 8 and 12 km.

Both figures show that the required threshold T has a huge effect on the coverage probability, but a limited effect on the optimal radius of BC area. In addition, results show that for shared spectrum scenario, increasing λ_{BS} pushes the optimal point towards smaller values. This effect is not as clear in scenario 2. The main reason could be that in Scenario 1, adding more UC BS add more interference to BC users, and consequently, limits the BC sub-network efficiency. Moreover, a comparison between the two plots shows that there is no significant difference between the two cases in terms of the optimal radius, and it is limited to a shift of around one kilometer in some cases.

Similar remarks could be concluded from Fig. 8a and 8b, showing the total system capacity as a function of r_b for the two values of UC BS density mentioned above. Both figures
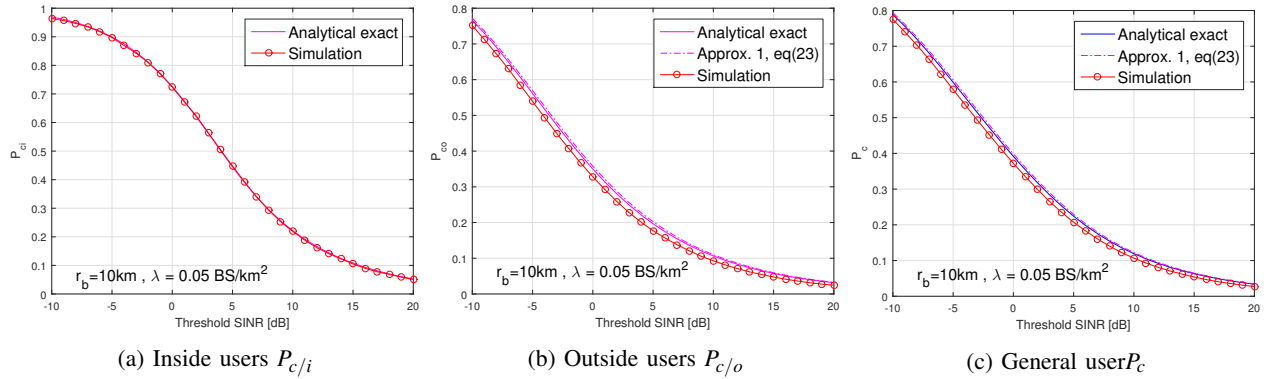
show that an optimal point can be determined for the set of parameters under test.

Since the average values, in general, could be misleading, and in order to highlight the effect of the position on the coverage, a test was done without the last averaging over position with respect to the center in Eq. (17) and (23) for Scenario 1, and Eq. (32) and (34) for Scenario 2. Fig. 9a and 9b show a cross-section of the service area, from the center to the edge, with the coverage probability at each point with distance R from the center of the service area, for two different values of λ_{BS}, and their corresponding optimal BC radius r_b for both scenarios. Results show that BC users have excellent coverage for both cases near the HPHT as expected, but this value drops dramatically for scenario 1 on the BC border due to interference, and the drop is more skewed when the density is higher. In the second scenario, the drop is smoother, and it is not affected by the density of BSs. Moreover, UC has a stable coverage value over most of its region except at both boundaries, with a higher average for higher density network, and with a slight outperformance for the dedicated spectrum scenario. One could mention the main changes in the BC/UC border region. In shared spectrum scenario, users on both sides of the UC/BC borders suffer from severe interference levels, which results in the gap seen in Fig.9a with a probability of coverage that drops down to 0.11 and 0.1 with λ_{BS} equal to 0.15 and $0.05BS/km^2$ respectively. In contrary, this gap is not as significant in Fig. 9b that corresponds to dedicated spectra scenario, as it is limited by the slight change in operating BSs density near the border.

Fig. 10a and 10b show the achievable capacity by 90% of the users in the service area for both scenarios. Higher UC network density achieves higher capacities, mainly due to the advantage of such networks in providing higher number of access points and then resources. Results also show that for shared spectrum scenario, a dense network requires smaller BC area to achieve its optimal values, while in dedicated spectra scenario, the density doesn't affect much the optimal point.

C. Effect of BS density

The second main design parameter for the hybrid network is the density of the BS providing unicast. To study the effect of the BS's density, probability of coverage, average user capacity, and average system capacity for inside, outside, and general user are calculated for different values of λ_{BS}, for both scenarios under study, for values of r_b around the optimal values found in the previous section, and are shown in Fig.11 and 12. For shared spectrum scenario, in general a low-density network will produce less interference on BC users, and thus those users will have better coverage and capacity. Nevertheless, low-density network means that UC users are on average far from their BS and thus have less coverage and capacity. The growth of coverage for UC users with the increase of λ_{BS} is faster than the decay of the coverage for BC users, thus the total coverage increases, until a point where further increase doesn't produce additional capacity or coverage since the interfering BSs are becoming closer to typical UC user. In the setting used here, one can conclude

(a) Inside users $P_{c/i}$ (b) Outside users $P_{c/o}$ (c) General user P_c
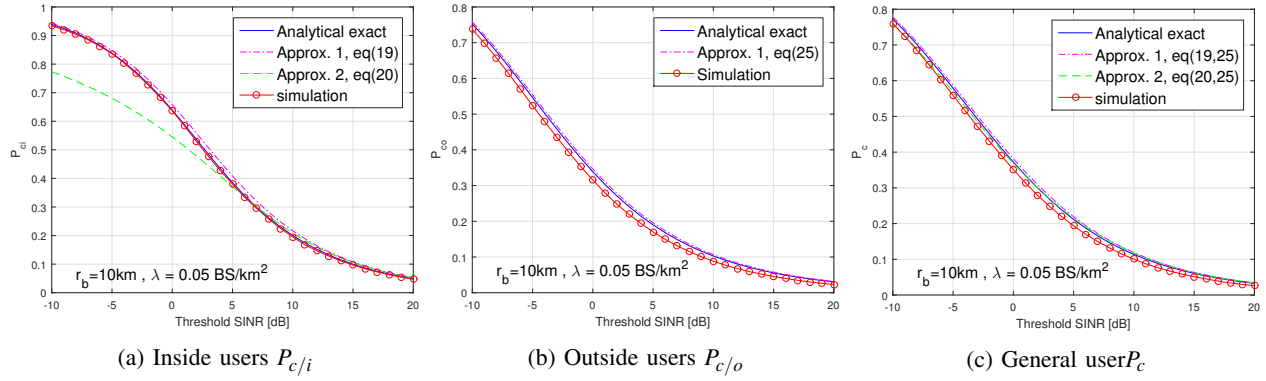
Fig. 5: CCDF of probability of coverage P_c for shared spectrum scenario

(a) Inside users $P_{c/i}$ (b) Outside users $P_{c/o}$ (c) General user P_c

Fig. 6: CCDF of probability of coverage P_c for dedicated spectra scenario

(a) Shared spectrum scenario   (b) Dedicated spectra scenario
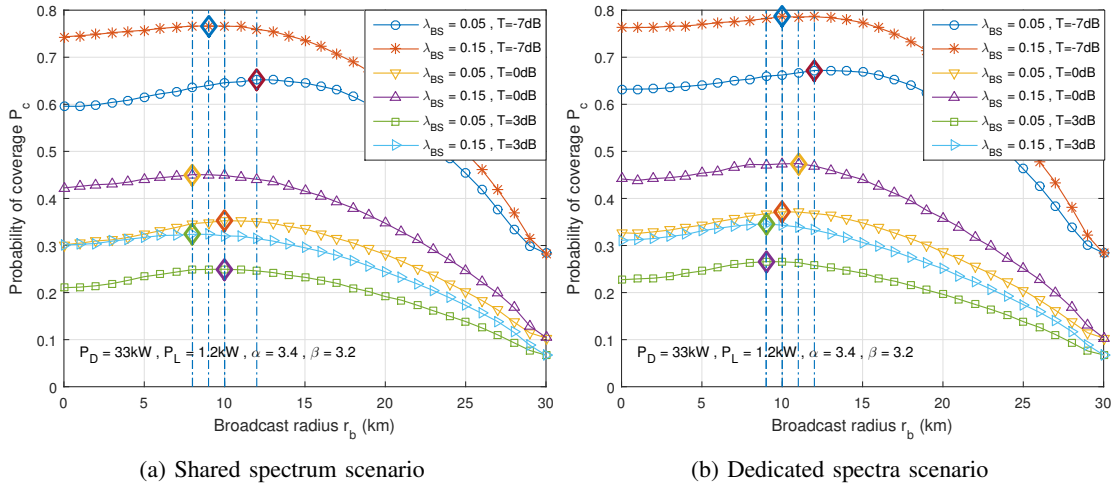
Fig. 7: Probability of coverage for both scenarios vs. the BC radius r_b for -100 dBm noise power

that $0.15BS/km^2$ is enough for nearly maximum coverage and $0.1BS/km^2$ for maximum user capacity.

Similarly, Fig. 11c and 12c shows the total average system capacity for the hybrid network as a function of UC BS density. The results have the same indication, a BS density equal to $0.15BS/km^2$ is enough to have optimal system capacity. In dedicated spectrum scenario, however, the density doesn't affect the inside users' capacity and coverage, and consequently the coverage, average user capacity, and average system capacity are higher in general. However, Scenario 2

doesn't significantly shift the value on which the coverage and capacity become stable. In practice, the control of BS density can be done by turning off the service transmission of selected BSs but this leads to a new model of a PPP network which is out-of-scope in this paper.

D. Interference cancellation

In all the testings performed so far, the induced interference was fully taken into account as no interference cancellation was supposed to be carried out. Here the effect of potential
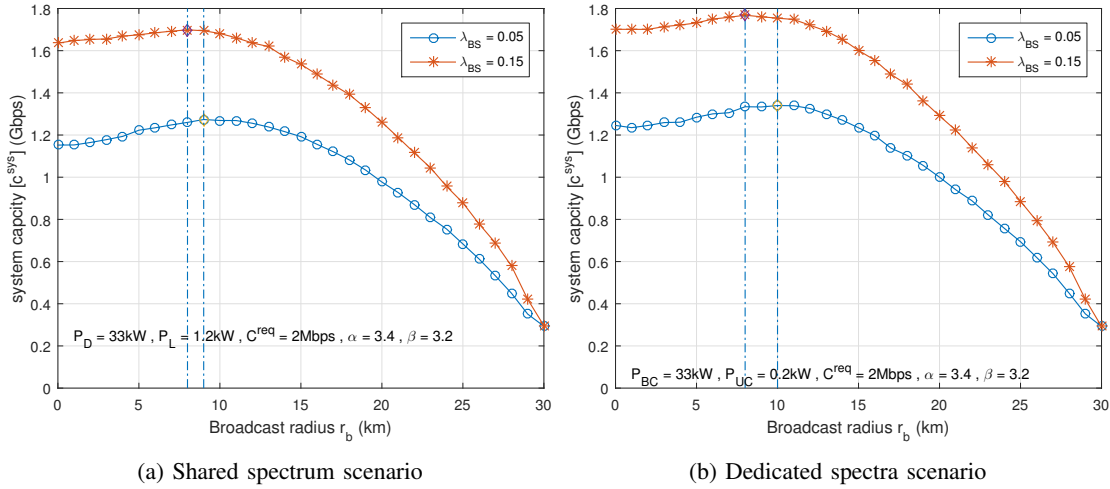
(a) Shared spectrum scenario

(b) Dedicated spectra scenario

Fig. 8: Average system capacity vs. the BC radius r_b for -100 dBm noise power, C^{req} of 2 Mbps, and 1400 users

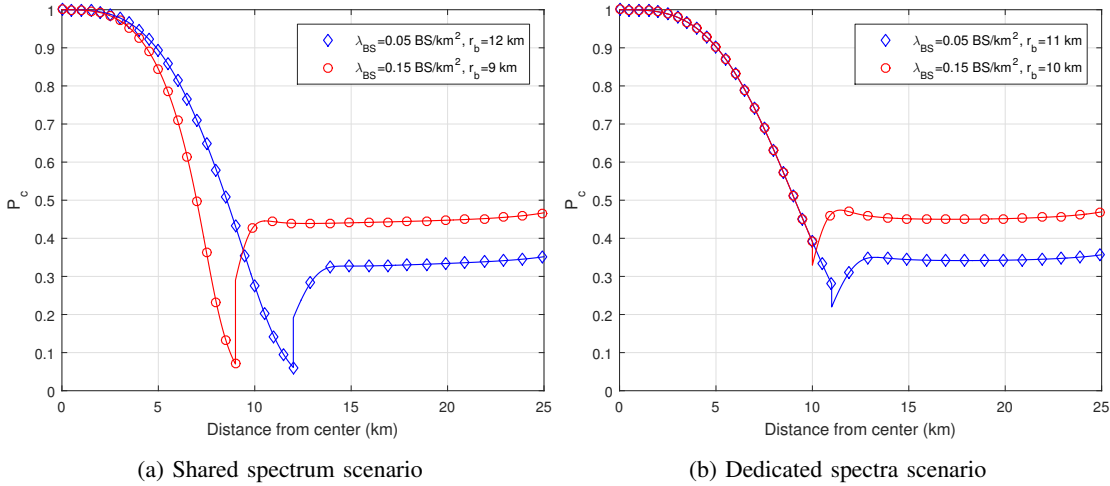(a) Shared spectrum scenario

(b) Dedicated spectra scenario

Fig. 9: Probability of coverage as a function of distance from center for two values of λ_{BS} and their corresponding values of r_b for $-100dBm$ noise power and T=0 dB
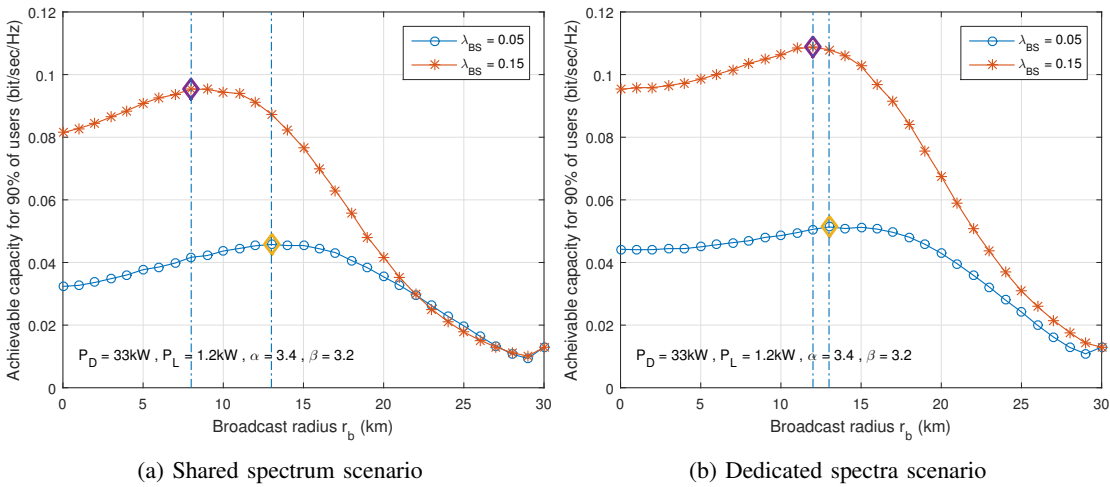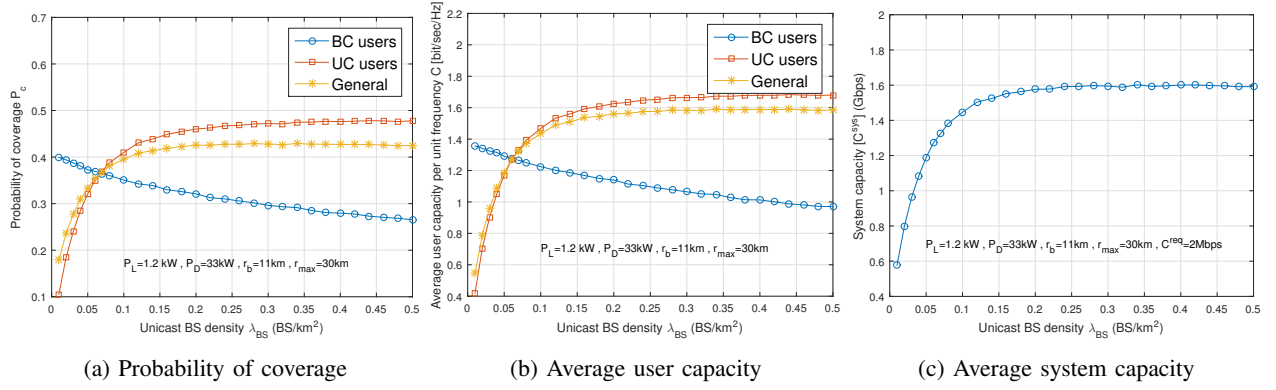

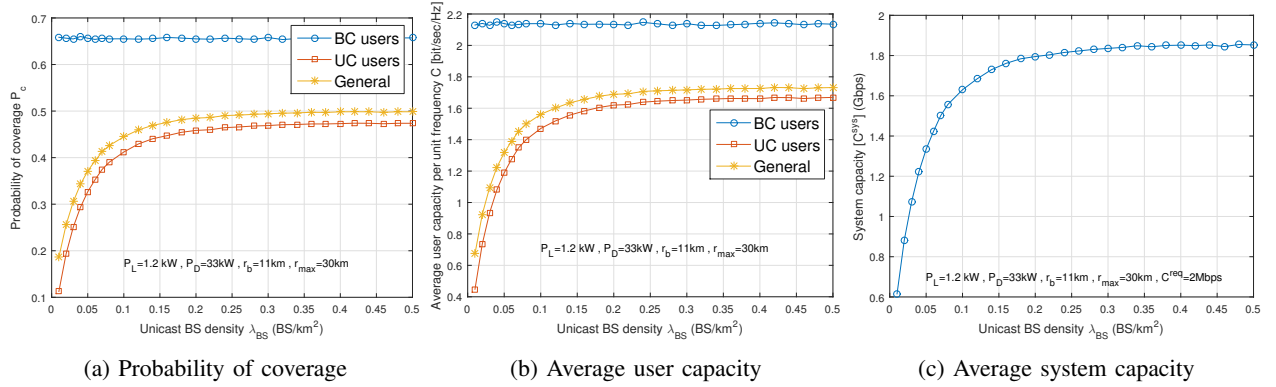(a) Shared spectrum scenario

(b) Dedicated spectra scenario

Fig. 10: Achievable user capacity per unit frequency vs. the BC radius r_b for -100 dBm noise power and T= 0 dB

interference cancellation technique, modeled with a cancellation factor γ is studied. In fact, the SINR formulas are slightly modified versions of Eq. (2) and Eq. (3) to include the new factor. For shared spectrum the modified formula for BC and

(a) Probability of coverage   (b) Average user capacity   (c) Average system capacity

Fig. 11: Effect of the BSs' density λ_{BS} for shared spectrum scenario

(a) Probability of coverage   (b) Average user capacity   (c) Average system capacity

Fig. 12: Effect of the BS's density λ_{BS} for dedicated spectra scenario

UC users will be respectively as following:

$$S_i = \frac{P_D g r_V^{-\beta}}{\sigma^2 + \gamma I_D} \tag{51}$$

and

$$S_o = \frac{P_L h r_l^{-\alpha}}{\sigma^2 + \gamma (I_1 + I_2)} \tag{52}$$

Similarly, for dedicated spectra scenario, SINR will be modified but with reduced effect. SINR of BC users will remain unchanged as in Eq. (7), while SINR of UC will be a modification of Eq. (8), and will be as following:

$$S_o = \frac{P_L h r_l^{-\alpha}}{\sigma^2 + \gamma (I_1)} \tag{53}$$

where γ is the reduction factor, and $\gamma \leq 1$. Fig. 13 and 14 show the coverage probability, average user capacity, and achievable capacity for shared spectrum scenario and dedicated spectra scenario respectively.

Fig. 13a and 14a show that for both scenarios, coverage could be enhanced by more than 67% for $\lambda = 0.15 BS/km^2$ and around 37% for $\lambda = 0.05 BS/km^2$ with a cancellation factor of -15 dB. Further cancellation increase, i.e. lower values of γ, will not be as effective as noise becomes the dominant limiting factor. The results show also that the 15 dB cancellation could achieve around 130% increase in average capacity for a user, and around 250% increase in achievable capacity for 90% of users.

E. Comparison between the two scenarios

The two presented scenarios share most of the design criteria, except the frequency bands occupied by each. While the difference in probability of coverage and system capacity is not significant, edge users in the two scenarios experience very different conditions as can be seen in Fig. 9a and 9b. As can be concluded from Fig. 5c and 6c for Coverage Probability and Fig. 8a and 8b for capacity, dedicated spectra scenario has a slight advantage due to fewer sources of interference. However, this slight advantage comes with a very expensive price in terms of occupied bandwidth, due to the use two frequency bands instead of one. For a fair comparison, let us analyze the two scenarios from the perspective of the global area spectral efficiency defined as

$$A_e = \frac{C^{sys}}{BW_{total} \, \pi r_{max}^2} \tag{54}$$

where $BW_{total} = BW_{BC} + BW_{UC}$ is the total bandwidth. $BW_{total} = 18$ MHz for the dedicated spectra scenario, and $BW_{total} = 10$ MHz in the case of shared spectrum scenario because of the overlapping of the bands. The global area spectral efficiency as a function of the BC radius is shown in Fig.15.

The results show that even though dedicated spectrum scenario achieves higher capacity and coverage, but globally, shared spectrum scenario is more efficient. The large distances between the HPHT and UC users from one side, and the BS and BC users from the other side, cause the mutual
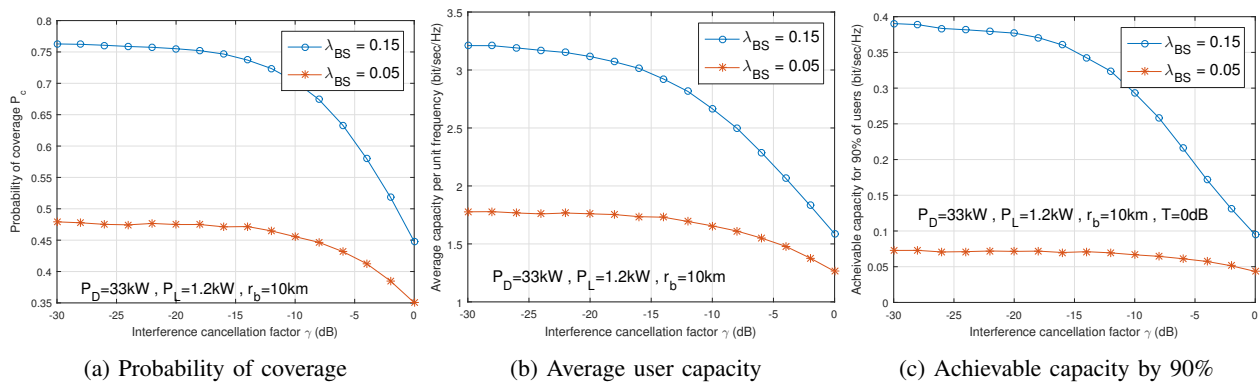
(a) Probability of coverage   (b) Average user capacity   (c) Achievable capacity by 90%

Fig. 13: Effect of interference cancellation factor γ on coverage and capacity for shared spectrum scenario

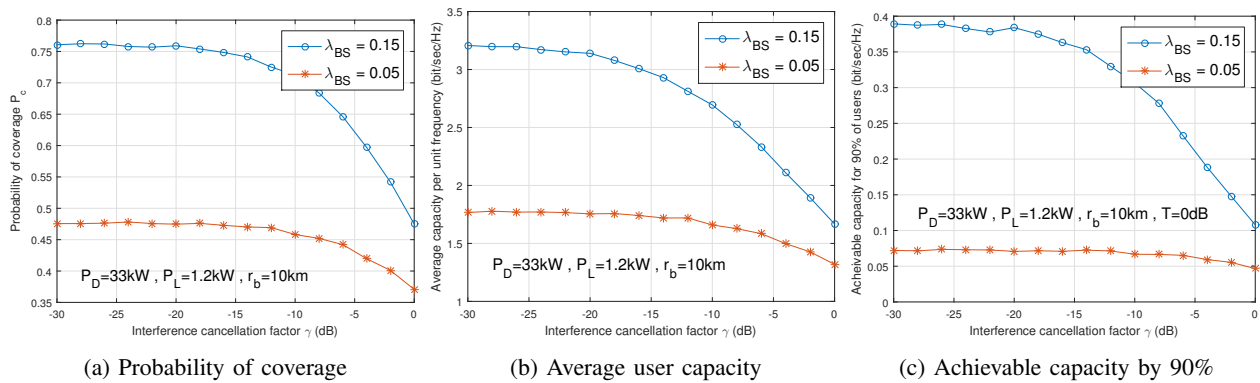(a) Probability of coverage   (b) Average user capacity   (c) Achievable capacity by 90%

Fig. 14: Effect of interference cancellation factor γ on coverage and capacity for dedicated spectra scenario
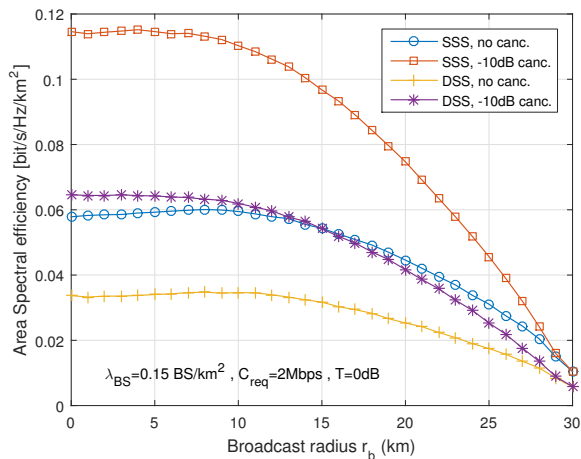

Fig. 15: Global area spectral efficiency comparison between the two proposed scenarios with and without interference cancellation (SSS=Shared Spectrum Scenario, DSS= Dedicated Spectra Scenario).

interference to be limited to the edge users. Hence, cancelling this interference by using dedicated spectra scenario has a limited effect on the average coverage and capacity, while the bandwidth used is hugely increased (doubled, or even more depending on the used networks) to attain such goal. This eventually leads to a severe drop of the efficiency in the second scenario. The results also show that dedicated

spectral scenario with -10 dB of interference cancellation can reach the efficiency level of shared spectrum scenario with no interference management. Moreover, It can be noticed that the use of more advanced receivers with better interference management has more effect on the shared spectrum scenario doubling the efficiency, whereas the effect on the dedicated spectra scenario is limited because of the fewer number of interference sources in that case.

However, it remains up to the designer to use either choice depending on the available resources and their cost. For example, if the state of the edge users is critical, and the additional BW is available and not costly, then dedicated spectra scenario could again be the preferable network option.

Table III briefs the comparison between the shared spectrum scenario (SSS) and the dedicated spectra scenario (DSS)

TABLE III: Comparison between the SSS and DSS scenarios

Parameter	SSS	DSS
Average coverage	slightly lower	slightly higher
Average capacity	slightly lower	slightly higher
Edge users coverage	very low coverage	better conditions
Used BW	single frequency band	double frequency band
Global spectral efficiency	much higher	much lower

VI. CONCLUSION

The work in this paper introduced two different models for hybrid broadcast/broadband coexistence. The first was based on shared spectrum access while the second was based on

dedicated spectrum using TVWS. An analytical formulation for both models in terms of probability of coverage and capacity has been derived, and numerical simulations have verified the accuracy of the derived expressions. To the best of the authors knowledge, this paper presents a first reference work dealing with the optimization of the hybrid network with the coexistence of broadband and broadcast networks, from stochastic geometry perspective, taking into account the inter cell interference.

The results showed that in general, the dedicated spectra scenario produces higher coverage probability for a user in the service area by few percents and higher system capacity as well, with similar percentages. However, since it requires an additional frequency band adopted from the TV white space, a compromise could be made between coverage and spectral resources. Even though the compromise, i.e. the choice of Scenario 1 or Scenario 2, could be hard to find, a soft solution where Scenario 1 is applied in general, but TV white space is used for BS on the BC/UC boundaries, can be proposed in the future.

The results also indicated that an optimal broadcast radius could be reached for different operation conditions where coverage or capacity could be maximized. The results showed that this optimal point changes depending on the density of UC BS. It is shown that, for both scenarios, a value of BS density beyond which there is no significant gain in either scenario exists. Moreover, it is shown that some interference cancellation possibly introduced at the end-user level could significantly enhance both coverage and user experience. The two proposed scenarios were also directly compared in terms of are spectral efficiency, where the shared spectrum scenario proved to be much more efficient.

The scenarios discussed here are one of many possible configurations. Future investigations on scenarios like broadcast/multi-cast hybrid network could be explored. Finally, it is expected to consider multi broadcast cells in future research directions.

APPENDIX A
USEFUL INTEGRATIONS

In the following derivations an integration on a plane for a function over a disk will be needed

A. Integration over a distinct disk

For a disk C with radius R, and with distance D from the origin, where $D > R$, the integration of function f over the plane could be given by:

$$\int_{C_{/D}} f(r) = \int_{D-R}^{D+R} 2\theta r f(r) dr \qquad (55)$$

By taking an arc strip with length as $2\theta r$ as shown in Fig. 16. According to cosine law:

$$\theta = \arccos\left(\frac{r^2 + D^2 - R^2}{2rD}\right) \qquad (56)$$

then the integration will finally be givan by:

$$\int_{C_{/D}} f(r) = \int_{D-R}^{D+R} 2\arccos\left(\frac{r^2 + D^2 - R^2}{2rD}\right) r f(r) dr \qquad (57)$$
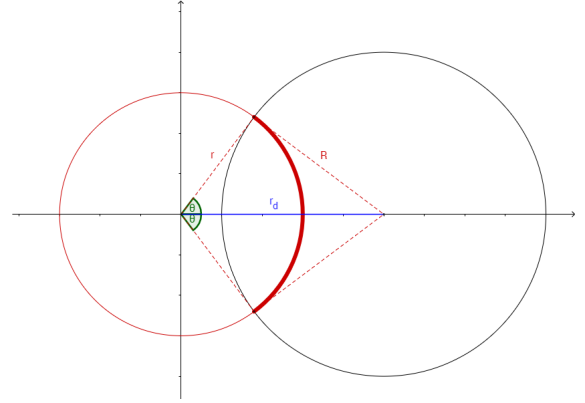

Fig. 16: integration over a distinct disk

B. Integration over a inscribing disk

For a disk C with radius R, and with distance D from the origin, where $D < R$, the integration of function f over the plane could be given by:

$$\int_{C_{/D}} f(r) = \int_{0}^{R-D} 2\pi r f(r) dr + \int_{R-D}^{R+D} 2\theta r f(r) dr \qquad (58)$$

where the first term corresponds to the integration of a circular strip from the origin until the strip hits the disk boundaries, and the second term corresponds to a strip starting from the end of first limit, to the end of the disk. this is shown in Fig. 17. Similar to the section above, the final integration will be:

$$\int_{C_{/D}} f(r) = \int_{0}^{R-D} 2\pi r f(r) dr + \int_{R-D}^{R+D} 2\arccos\left(\frac{r^2 + D^2 - R^2}{2rD}\right) r f(r) dr \qquad (59)$$
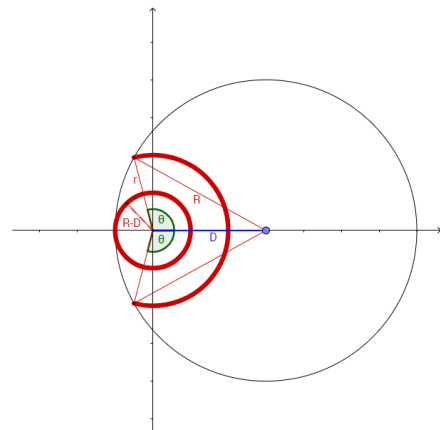

Fig. 17: integration over a inscribing disk

APPENDIX B
CALCULATION OF $\mathscr{L}_{I_D}$

The term $\mathscr{L}_{I_D/r_v}(s)$ could be evaluated as follows:

$$
\begin{aligned}
\mathscr{L}_{I_D/r_v}(s) &= \mathbb{E}[\exp(-sI_D)] \\
&= \mathbb{E}_{\Phi,h}[\exp(-s\sum_{j\in\Phi}P_L h r_{s,j}^{-\alpha})] \\
&\overset{(a)}{=} \mathbb{E}_{\Phi}\Big[\prod_j \mathbb{E}_h[\exp(-sP_L h r_{s,j}^{-\alpha})]\Big] \\
&\overset{(b)}{=} \mathbb{E}_{\Phi}\Big[\prod_j \frac{1}{1+\frac{sP_L}{\mu r_s^\alpha}}\Big] \\
&\overset{(c)}{=} exp(-\lambda\int_{\mathscr{O}\backslash\mathscr{G}}1-\frac{1}{1+\frac{sP_L}{\mu r_s^\alpha}}) \\
&\overset{(d)}{=} exp(-\lambda\int_{\mathscr{O}\backslash\mathscr{G}}\frac{1}{1+\frac{\mu r_s^\alpha}{sP_L}}) \\
&= exp\Big(\underbrace{-\lambda\int_{\mathscr{O}}\frac{1}{1+\frac{\mu r_s^\alpha}{sP_L}}}_{term1}+\underbrace{\lambda\int_{\mathscr{G}}\frac{1}{1+\frac{\mu r_s^\alpha}{sP_L}}}_{term2}\Big)
\end{aligned}
\tag{60}
$$

where (a) follows the independence of channel effect h from the point process Φ. (b) follows the assumed exponential distribution of h: $h\sim exp(\mu)$, and that if x is exponentially distributed random variable with parameter θ then $\mathbb{E}_x[\exp(-ax)]=\frac{1}{1+(a/\theta)}$,and (c) follows the probability generating functional (PGFL) of the PPP. The integration at (c) is done over the unicast area, *i.e.* over the whole service area $\mathscr{O}$, excluding the broadcast area, or the gap $\mathscr{G}$. *term*1 corresponds to interference hypothetically produced by BSs distributed over the whole service area¿ However, since BSs inside the BC area operate at different frequency, thus not interfering with the users received signal, a gap in the uniformly distributed interferes appears, and this is managed by *term*2. The latter corresponds to this gap in interfering BSs' distribution. Since the integrations in both terms are on an inscribing disk the method described in appendix A, part B, could be used to calculate *terms*1 and *term*2 as following:

$$
term1 = -2\lambda\Big(\int_0^{r_{max}-r_v}\frac{\pi r_s}{1+\frac{\mu r_s^\alpha}{sP_L}}dr_s+\int_{r_{max}-r_v}^{r_{max}+r_v}\frac{\arccos(\frac{r_v^2+r_s^2-r_{max}^2}{2r_v r_s})}{1+\frac{\mu r_s^\alpha}{sP_L}}r_s dr_s\Big)
\tag{61}
$$

$$
term2 = 2\lambda\Big(\int_0^{r_b-r_v}\frac{\pi r_s}{1+\frac{\mu r_s^\alpha}{sP_L}}dr_s+\int_{r_b-r_v}^{r_b+r_v}\frac{\arccos(\frac{r_v^2+r_s^2-r_b^2}{2r_v r_s})}{1+\frac{\mu r_s^\alpha}{sP_L}}r_s dr_s\Big)
\tag{62}
$$

Plugging *term*1 and *term*2 into (60), and substituting s by its value, we then have:

$$
\begin{aligned}
\mathscr{L}_{I_D/r_v}(\frac{\tau T r_v^\beta}{P_D}) = \exp\Big(-2\lambda\Big(&\int_0^{r_{max}-r_v}\frac{\pi r_s}{1+\frac{\mu P_D r_s^\alpha}{T\tau P_L r_b^\beta}}dr_s \\
&+\int_{r_{max}-r_v}^{r_{max}+r_v}\frac{\arccos(\frac{r_v^2+r_s^2-r_{max}^2}{2r_v r_s})}{1+\frac{\mu P_D r_s^\alpha}{T\tau P_L r_b^\beta}}r_s dr_s \\
&-\int_0^{r_b-r_v}\frac{\pi r_s}{1+\frac{\mu P_D r_s^\alpha}{T\tau P_L r_b^\beta}}dr_s \\
&-\int_{r_b-r_v}^{r_b+r_v}\frac{\arccos(\frac{r_v^2+r_s^2-r_b^2}{2r_v r_s})}{1+\frac{\mu P_D r_s^\alpha}{T\tau P_L r_b^\beta}}r_s dr_s\Big)\Big)
\end{aligned}
$$

First approximation follows the same procedure in Eq. (60) until (d). next step will be by similar yet opposite approach as in appendix A part (B), integrate over the disk of radius r_v and trimmed by the BC disk, this will produce Eq. (19).

As for second approximation, the steps are as following:

$$
\begin{aligned}
\mathscr{L}^{**}_{I_D/r_v}(s) &= \mathbb{E}[\exp(-sI_D)] \\
&= \mathbb{E}_h[\exp(-sP_L h(r_b-r_v)^{-\alpha})] \\
&= \frac{1}{1+\frac{sP_L}{\mu(r_b-r_v)^\alpha}}
\end{aligned}
\tag{63}
$$

Finally, substituting s by its value, will produce formula in (20)

APPENDIX C
CALCULATION OF $\mathscr{L}_{I_1}$

$\mathscr{L}_{I_1/r_d}(s)$ could be calculated as following:

$$
\begin{aligned}
\mathscr{L}_{I_1/r_d}\Big(s\Big) &= \mathbb{E}_{\Phi,h}\Big[\exp\Big(-s\sum_{j\in\Phi/b}P_L h r_{q,j}^{-\alpha}\Big)\Big] \\
&= \mathbb{E}_{\Phi}\Big[\prod_{j\in\Phi/b}\mathbb{E}_h\big[\exp\big(-sP_L h r_{q,j}^{-\alpha}\big)\big]\Big] \\
&= \mathbb{E}_{\Phi}\Big[\prod_{j\in\Phi/b}\frac{1}{1+\frac{sP_L r_q^{-\alpha}}{\mu}}\Big] \\
&\overset{(a)}{=} \exp\Big(-\lambda\int_{\mathscr{O}\backslash\mathscr{G}}1-\frac{1}{1+\frac{sP_L r_q^{-\alpha}}{\mu}}dr_q\Big) \\
&= \exp\Big(-\lambda\int_{\mathscr{O}\backslash\mathscr{G}}\frac{1}{1+\frac{\mu r_q^\alpha}{sP_L}}dr_q\Big) \\
&= \exp\Big(\underbrace{-\lambda\int_{\mathscr{O}}\frac{1}{1+\frac{\mu r_q^\alpha}{sP_L}}dr_q}_{term1}+\underbrace{\lambda\int_{\mathscr{G}}\frac{1}{1+\frac{\mu r_q^\alpha}{sP_L}}dr_q}_{term2}\Big)
\end{aligned}
\tag{64}
$$

where (a) also follows the PGFL of the PPP. *term*1 refers to the interference generated by the whole service area with uniformly distributed BSs, and *term*2 refers to the gap caused by the absence of interferers in the BC area. *term*1 integrates over inscribing disk, then the method in appendix A, part (B) is applied to formulate it as following:

$$term1 = -\lambda \Bigg(\int_{min(r_l,r_{max}-r_d)}^{r_{max}-r_d} \frac{2\pi r_q}{1+\frac{\mu r_q^\alpha}{sP_L}} dr_q$$
$$+ \int_{max(r_l,r_{max}-r_d)}^{r_{max}+r_d} \frac{2\arccos(\frac{r_d^2+r_q^2-r_{max}^2}{2r_d r_q})}{1+\frac{\mu r_q^\alpha}{sP_L}} r_q dr_q \Bigg) \quad (65)$$

$term2$ integrates over a distinct disk (the gap), and the method in appendix A, part (A) is used to formulate it as following:

$$term2 = \lambda \int_{max(r_l,r_d-r_b)}^{r_d+r_b} \frac{2\arccos(\frac{r_d^2+r_q^2-r_b^2}{2r_d r_q})}{1+\frac{\mu r_q^\alpha}{sP_L}} r_q dr_q \quad (66)$$

then, by substituting s by its value we have:

$$\mathscr{L}_{I_1/r_d}\left(\frac{\mu T r_l^\alpha}{P_L}\right) = \exp\Bigg(-2\lambda \Bigg(\int_{min(r_l,r_{max}-r_d)}^{r_{max}-r_d} \frac{\pi r_q}{1+\frac{1}{T}\left(\frac{r_q}{r_l}\right)^\alpha} dr_q$$
$$+ \int_{max(r_l,r_{max}-r_d)}^{r_{max}+r_d} \frac{\arccos(\frac{r_d^2+r_q^2-r_{max}^2}{2r_d r_q})}{1+\frac{1}{T}\left(\frac{r_q}{r_l}\right)^\alpha} r_q dr_q$$
$$- \int_{max(r_l,r_d-r_b)}^{r_d+r_b} \frac{\arccos(\frac{r_d^2+r_q^2-r_b^2}{2r_d r_q})}{1+\frac{1}{T}\left(\frac{r_q}{r_l}\right)^\alpha} r_q dr_q \Bigg) \Bigg) \quad (67)$$

ACKNOWLEDGMENT

REFERENCES

[1] Research and Markets, *Global Mobile TV Market Size, Market Share, Application Analysis, Regional Outlook, Growth Trends, Key Players, Competitive Strategies and Forecasts, 2017 to 2025*, 2017.

[2] C. Wong, G. Wei-Han Tan, T.n Hew, and K.n Ooi, "Can mobile tv be a new revolution in the television industry?," *Computers in Human Behavior*, vol. 55, no. Part B, pp. 764 – 776, 2016.

[3] M. El-Hajjar and L. Hanzo, "A survey of digital television broadcast transmission techniques," *IEEE Communications Surveys Tutorials*, vol. 15, no. 4, pp. 1924–1949, 2013.

[4] L. Fay, L. Michael, D. Gmez-Barquero, N. Ammar, and M. W. Caldwell, "An overview of the atsc 3.0 physical layer specification," *IEEE Transactions on Broadcasting*, vol. 62, no. 1, pp. 159–171, 2016.

[5] A. Yamada, H. Matsuoka, T. Ohya, R. Kitahara, J. Hagiwara, and T. Morizumi, "Overview of isdb-tmm services and technologies," in *2011 IEEE International Symposium on Broadband Multimedia Systems and Broadcasting (BMSB)*, 2011, pp. 1–5.

[6] F. Luo, *Mobile Multimedia roadcasting tandards*, 2009.

[7] "3gpp lte"," http://www.3gpp.org/technologies/keywords-acronyms/98-lte," .

[8] F. Hartung, U. Horn, J. Huschke, M. Kampmann, T. Lohmar, and M. Lundevall, "Delivery of broadcast services in 3g networks," *IEEE Transactions on Broadcasting*, vol. 53, no. 1, pp. 188–199, 2007.

[9] F. Hartung, U. Horn, J. Huschke, M. Kampmann, and T. Lohmar, "Mbmsip multicast/broadcast in 3g networks," *International Journal of Digital Multimedia Broadcasting*, vol. 2009, 2009.

[10] D. Lecompte and F. Gabin, "Evolved multimedia broadcast/multicast service (embms) in lte-advanced: overview and rel-11 enhancements," *IEEE Communications Magazine*, vol. 50, no. 11, pp. 68–74, 2012.

[11] L. Christodoulou, O. Abdul-Hameed, and A. M. Kondoz, "Toward an lte hybrid unicast broadcast content delivery framework," *IEEE Transactions on Broadcasting*, vol. PP, no. 99, pp. 1–17, 2017.

[12] H. Voigt, "Hybrid media and tv delivery using mobile broadband combined with terrestrial/satellite tv," in *Electronics Conference Biennial Baltic. 15TH*, 2016.

[13] P. A. Fam, M. Crussière, J. F. Hélard, P. Bretillon, and S. Paquelet, "Global throughput maximization of a hybrid unicast-broadcast network for linear services," in *2015 International Symposium on Wireless Communication Systems (ISWCS)*, 2015, pp. 146–150.

[14] J. Calabuig, J. F. Monserrat, and D. Gmez-Barquero, "5th generation mobile networks: A new opportunity for the convergence of mobile broadband and broadcast services," *IEEE Communications Magazine*, vol. 53, no. 2, pp. 198–205, 2015.

[15] C. Singhal and S. De, "Energy-efficient and qoe-aware tv broadcast in next-generation heterogeneous networks," *IEEE Communications Magazine*, vol. 54, no. 12, pp. 142–150, 2016.

[16] P. Unger and T. Krner, "Modeling and performance analyses of hybrid cellular and broadcasting networks," *International Journal of Digital Multimedia Broadcasting*, vol. 2009, 2009.

[17] C. Heuck, "An analytical approach for performance evaluation of hybrid (broadcast/mobile) networks," *IEEE Transactions on Broadcasting*, vol. 56, no. 1, pp. 9–18, 2010.

[18] K. Wang, Z. Chen, and H. Liu, "Push-based wireless converged networks for massive multimedia content delivery," *IEEE Transactions on Wireless Communications*, vol. 13, no. 5, pp. 2894–2905, 2014.

[19] A. Lykourgiotis, K. Birkos, T. Dagiuklas, E. Ekmekcioglu, S. Dogan, Y. Yildiz, I. Politis, G. O. Tanik, B. Demirtas, A. M. Kondoz, and S. Kotsopoulos, "Hybrid broadcast and broadband networks convergence for immersive tv applications," *IEEE Wireless Communications*, vol. 21, no. 3, pp. 62–69, 2014.

[20] N. Cornillet, M. Crussière, and J. F. Hélard, "On the hybrid use of unicast/broadcast networks under energy criterion," in *2012 IEEE 23rd International Symposium on Personal, Indoor and Mobile Radio Communications - (PIMRC)*, 2012, pp. 1256–1261.

[21] L. Polak, D. Plaisner, O. Kaller, J. Milos, and T. Kratochvil, "Co-existence between dvb-t2-lite and lte downlink networks in advanced mobile fading channels - partial overlapping rf spectrum," in *2016 39th International Conference on Telecommunications and Signal Processing (TSP)*, 2016, pp. 458–461.

[22] I. Cho, I. Lee, and Y. Park, "Study on coexistence between long term evolution and digital broadcasting services," *International Journal of Advanced Science and Technology*, vol. 38, pp. 75–92, 2012.

[23] M. Crussière, C. Douillard, C. Gallard, M. Le Bot, B. Ros, A. Bouttier, and A. Untersee, "A unified broadcast layer for horizon 2020 delivery of multimedia services," *IEEE Transactions on Broadcasting*, vol. 60, no. 2, pp. 193–207, 2014.

[24] D. Rother, S. Ilsen, and F. Juretzek, "A software defined radio based implementation of the tower overlay over lte-a+ system," in *Broadband Multimedia Systems and Broadcasting (BMSB), 2014 IEEE International Symposium on*. IEEE, 2014, pp. 1–6.

[25] H. Bawab, P. Mary, J. F. Hélard, Y. Nasser, and O. Bazzi, "Global ergodic capacity closed-form expression of coexisting dvb-lte-like systems," in *2014 IEEE 79th Vehicular Technology Conference (VTC Spring)*, 2014, pp. 1–5.

[26] A. A. Razzac, S. E. Elayoubi, T. Chahed, and B. El Hassan, "Planning of mobile tv service in standalone and cooperative dvb-ngh and lte networks," in *2013 11th International Symposium and Workshops on Modeling and Optimization in Mobile, Ad Hoc and Wireless Networks (WiOpt)*, 2013, pp. 609–614.

[27] A. A. Razzac, S. E. Elayoubi, T. Chahed, and B. El-Hassan, "Comparison of lte embms and dvb-ngh mobile tv solutions from an energy consumption perspective," in *2013 IEEE 24th International Symposium on Personal, Indoor and Mobile Radio Communications (PIMRC Workshops)*, 2013, pp. 16–20.

[28] P. A. Fam, S. Paquelet, M. Crussière, J. F. Hélard, and P. Bretillon, "Optimal capacity of hybrid unicast-broadcast networks for mobile tv services," in *2016 IEEE International Symposium on Broadband Multimedia Systems and Broadcasting (BMSB)*, 2016, pp. 1–5.

[29] P. A. Fam, S. Paquelet, M. Crussière, J. F. Hélard, and P. Bretillon, "Analytical derivation and optimization of a hybrid unicast-broadcast network for linear services," *IEEE Transactions on Broadcasting*, vol. 62, no. 4, pp. 890–902, 2016.

[30] P. A. Fam, S. Paquelet, M. Crussière, J. F. Hélard, and P. Bretillon, "On the energy efficiency of hybrid unicast-broadcast networks for mobile tv services," *Journee Scientifique URSI-France 2016 Energie et Radiosciences*, 2016.

[31] M.Haenggi, *Stochastic geometry for wireless networks*, Cambridge University Press, 2012.

[32] M. Haenggi, J. G. Andrews, F. Baccelli, O. Dousse, and M. Franceschetti, "Stochastic geometry and random graphs for the analysis and design of wireless networks," *IEEE Journal on Selected Areas in Communications*, vol. 27, no. 7, pp. 1029–1046, September 2009.

[33] F. Baccelli, M. Klein, M. Lebourges, and S. Zuyev, "Stochastic geometry and architecture of communication networks," *PTelecommunication Systems*, vol. 7, no. 1, pp. 209–227, 1997.

[34] W. Lu and M. Di Renzo, "Stochastic geometry modeling of cellular networks: Analysis, simulation and experimental validation," in *Proceedings of the 18th ACM International Conference on Modeling, Analysis and Simulation of Wireless and Mobile Systems*. 2015, MSWiM '15, pp. 179–188, ACM.

[35] J. G. Andrews, F. Baccelli, and R. K. Ganti, "A tractable approach to coverage and rate in cellular networks," *IEEE Transactions on Communications*, vol. 59, no. 11, pp. 3122–3134, 2011.

[36] A.Shokair, Y. Nasser, O. Bazzi, J.F. Hélard, and M. Crussière, "Near optimal linear-service oriented resource allocation strategy for lte networks," in *The 9th International Congress on Ultra Modern Telecommunications and control systems ICUMT*, 2017.

[37] G. Ryzhik and T. Geronimus, *Table of Integrals, Series, and Products, seventh edition*, Academic Press, 2007.